in Scheme II is consistent with the latest values for the Mn^+–H and Mn^+–CH_3 bond energies.[2f,g] By using these values and average bond energies for (CH_2)–H and (CH_2)–CH_3 bonds, we estimate an upper limit on strain energy for the manganese–cycloheptyne species **14** of **18** kcal/mol.

The Mn^+-induced demethanation across the triple bond of acetylenes is also reflected if one generates Mn(alkyne)$^+$ complexes with shorter alkyl chain length. This can be clearly seen from the data of the Mn(alkyne)$^+$ complexes given in Table II. While CH_4 loss is found for both **10** and **16**, the reaction is not observed for **17** and **18**. This is, presumably, a direct consequence of the fact that for smaller alkynes the formation of metallacycles analogous to **14** is no longer possible. Instead, reactions dominate in which either the ligand is detached from the Mn(alkyne)$^+$ complex or processes occur which involve the C_3H_7 unit (loss of H_2 and C_2H_4) only.

Conclusions

In contrast to previous reports, Mn^+ is not necessarily an unreactive transition metal ion in the gas phase. In the present system its reactivity with alkynes is even higher than that of the analogous Fe(alkyne)$^+$ complexes which were previously throught of having the highest reactivity. Our results imply that either the hitherto used concepts for the oxidative addition of CX bonds to transition metal ions deserve a reconsideration of, alternatively, that the Mn^+ ions generated upon both electron impact (EI) and fast atom bombardment (FAB) are electronically excited, thus generating reactive species. While the formation of electronically excited Mn^+ upon electron impact ionization has been reported earlier,[2f,g,18] this possibility has not yet been considered for the FAB experiments.[2d,12] The identical behavior of the Mn(4-octyne)$^+$ complexes, generated via EI or FAB, strongly suggests that metal ions of the same electronic state distribution are formed, in which the excited ones are likely to cause the CH and CC activation.[18]

Mn^+-induced demethanation of 4-octyne follows to >83% a formal 1,6-elimination.[19] This unprecedented result could be interpreted by the formation of as yet unknown metallacycloalkyne intermediates. The study of labeled isotopomers and of the effects of chain length is in keeping with this interpretation.

Acknowledgment. We gratefully acknowledge support of our work by the following institutions: Deutsche Forschungsgemeinschaft, Fonds der Chemischen Industrie, Stiftung Volkswagenwerk, and Technische Universität Berlin.

Registry No. 10, 1942-45-6; **10a**, 108686-71-1; **10b**, 108686-72-2; **10c**, 81186-40-5; **10d**, 108686-73-3; **16**, 2586-89-2; **17**, 764-35-2; **18**, 107-00-6; $Mn(CO)_3(CH_3$-c-$C_5H_4)$, 12108-13-3; $Mn_2(CO)_{10}$, 10170-69-1; Mn^+, 14127-69-6; CH_4, 74-82-8; CH_3D, 676-49-3; CHD_3, 676-80-2; H_2, 1333-74-0; C_2H_4, 74-85-1; C_3H_4, 74-99-7; C_3H_6, 115-07-1.

(18) Beauchamp et al. (Halle, L. F.; Armentrout, P. B.; Beauchamp, J. L. *J. Am. Chem. Soc.* **1981**, *103*, 962) mention very briefly in a footnote that the reactivity of excited-state Mn^+ (produced by electron impact of $Mn_2(CO)_{10}$) with alkanes differs markedly from the reactions of ground-state ions.

(19) Co(*I*)-induced 1,5-demethanation of *n*-hexane does not, as interpreted by Allison (ref 1c), result in the formation of a saturated cobalt metallacycle. Instead, deuterium-labeling data are interpreted in the original paper[6] in terms of the conventional reaction sequence, i.e., a combination of CC and CH insertion reactions, thereby bypassing high oxidation states of Co^+.

Chemisorption on Size-Selected Metal Clusters: Activation Barriers and Chemical Reactions for Deuterium on Aluminum Cluster Ions

Martin F. Jarrold* and J. Eric Bower

Contribution from AT&T Bell Laboratories, Murray Hill, New Jersey 07974.
Received July 6, 1987

Abstract: We describe a new approach to investigating chemisorption on size-selected metal clusters. This approach involves investigating the collision-energy dependence of chemisorption using low-energy ion beam techniques. The method provides a direct measure of the activation barrier for chemisorption and in some cases an estimate of the desorption energy as well. We describe the application of this technique to chemisorption of deuterium on size-selected aluminum clusters. The activation barriers increase with cluster size (from a little over 1 eV for Al_{10}^+ to around 2 eV for Al_{27}^+) and show significant odd–even oscillations. The activation barriers for the clusters with an odd number of atoms are larger than those for the even-numbered clusters. In addition to chemisorption of deuterium onto the clusters, chemical reactions were observed, often resulting in cluster fragmentation. The main products observed were $Al_{n-1}D^+$, Al_{n-2}^+, and Al^+ for clusters with $n < 10$, and Al_nD^+ and $Al_{n-1}D^+$ for the larger clusters.

I. Introduction

Metal clusters might be considered as microscopic surfaces, and while there is an obvious relationship between chemisorption on surfaces and on bare metal clusters, we might anticipate that size, electronic properties, and geometric structure could influence chemisorption on the clusters. Since the application of the fast-flow reactor techniques to studying the chemistry of metal clusters[1-3] many cases have been identified in which the reaction rates show a strong cluster-size dependence. Several attempts have been made to account for these changes in reactivity, invoking either the electronic properties[4-7] or geometric structure.[8] The cluster-size dependence presumably results from changes in the height of the activation barrier associated with chemisorption, or changes in the stability of the adduct. However, it is often difficult to determine which of these factors is responsible.

(1) Riley, S. J.; Parks, E. K.; Nieman, G. C.; Pobo, L. C.; Wexler, S. *J. Chem. Phys.* **1984**, *80*, 1360. Richtsmeier, S. C.; Parks, E. K.; Liu, K.; Pobo, L. G.; Riley, S. J. *Ibid.* **1985**, *82*, 3659.

(2) Geusic, M. E.; Morse, M. D.; Smalley, R. E. *Rev. Sci. Instrum.* **1985**, *56*, 2123. Morse, M. D.; Geusic, M. E.; Heath, J. R.; Smalley, R. E. *J. Chem. Phys.* **1985**, *83*, 2293.

(3) Trevor, D. J.; Whetten, R. L.; Cox, D. M.; Kaldor, A. *J. Am. Chem. Soc.* **1985**, *107*, 518. Whetten, R. L.; Cox, D. M.; Trevor, D. J.; Kaldor, A. *J. Phys. Chem.* **1985**, *89*, 566.

(4) Whetten, R. L.; Cox, D. M.; Trevor, D. J.; Kaldor, A. *Phys. Rev. Lett.* **1985**, *54*, 1494.

(5) Trevor, D. J.; Kaldor, A. In *High Energy Processes in Organometallic Chemistry*; Suslick, K. S., Ed.; ACS Symposium Series; American Chemical Society: Washington, D.C., 1987.

(6) Upton, T. H. *Phys. Rev. Lett.* **1986**, *56*, 2168.

(7) Upton, T. H.; Cox, D. M.; Kaldor, A. In *The Physics and Chemistry of Small Clusters*; Jena, P., Ed.; Plenum: New York, 1987.

(8) Phillips, J. C. *J. Chem. Phys.* **1986**, *84*, 1951.

0002-7863/88/1510-0070$01.50/0

In this paper we describe a new approach to investigating chemisorption on metal clusters. Low-energy ion beam techniques are used to probe the collision-energy dependence of the chemisorption of a molecule onto a size-selected metal cluster ion. The resulting adduct (which we term a metastable adduct because it contains sufficient energy to dissociate back to reactants) is directly monitored using mass spectrometry. The collision-energy dependence of metastable adduct formation provides a measure of the activation barrier for chemisorption. Because the adduct is directly observed in these experiments, the collision-energy thresholds can be unambiguously related to the activation barrier for chemisorption. This is not true for the kinetic-energy thresholds of chemical reactions, where without prior thermodynamic information, the threshold could be due to reaction endothermicity or an activation barrier.

We report in this paper measurements of the activation barriers for chemisorption of deuterium (D_2) onto size-selected aluminum cluster ions containing between 10 and 27 atoms. We also report data on the chemical reactions of deuterium with the aluminum cluster ions. These reactions result in a number of products, often involving cluster fragmentation.

Chemisorption of hydrogen on neutral aluminum clusters has been investigated by the group at Exxon[7] using the fast-flow reactor technique. They found significant Al_nH_2 product only for Al_6 and Al_7. Upton[6,7] has suggested that Al_6 is the smallest cluster able to activate the hydrogen molecule and proposes a mechanism in which the hydrogen molecule approaches the cluster across one of the eight edges of the octahedral Al_6. Since chemisorption of hydrogen on polycrystalline aluminum has not been observed (although physisorption occurs at low temperatures[9,10]) the failure to observe chemisorption on the larger clusters might reflect the emergence of bulk properties. However, the cluster behavior has not been satisfactorily explained.

Experiments quite closely related to the ones described here have recently been performed by Anderson and co-workers[11] and Woste and co-workers.[12] Anderson and co-workers measured kinetic-energy thresholds for the reactions between small aluminum clusters Al_2^+–Al_8^+ and oxygen. Woste and co-workers have investigated the formation of $Ni_n(CO)_m^+$ species in sequential association reactions between mass-selected nickel cluster ions and CO.

II. Experimental Methods

The experimental methods have recently been described in detail[13,14] so only the main features will be reviewed here. The clusters are generated by pulsed laser vaporization of an aluminum rod in a continuous flow of helium buffer gas. The entire source is cooled to around −135 °C to promote the clustering processes. The clusters are ionized by a 1.5-kV electron beam and the clusters and buffer gas then expand into the vacuum chamber. After exiting the source the cluster ions are focused into a quadrupole mass spectrometer where the cluster ion of interest is selected. The size-selected cluster ions are then focused into a low-energy ion beam (of variable energy) and passed through a gas cell (which is at room temperature) where deuterium is introduced. The deuterium (Linde, CP grade) was further purified by an oxygen and water trap. After exiting the gas cell the reactant and product ions are focused into a second quadrupole mass spectrometer where they are analyzed. The ions are then detected by an off-axis collision dynode and an electron multiplier.

III. Results

There are two closely related aspects to the work described here: the chemical reactions between the aluminum clusters and deuterium (D_2), and chemisorption of deuterium onto the clusters to give the metastable $Al_nD_2^+$ adduct. We start by discussing the chemical reactions.

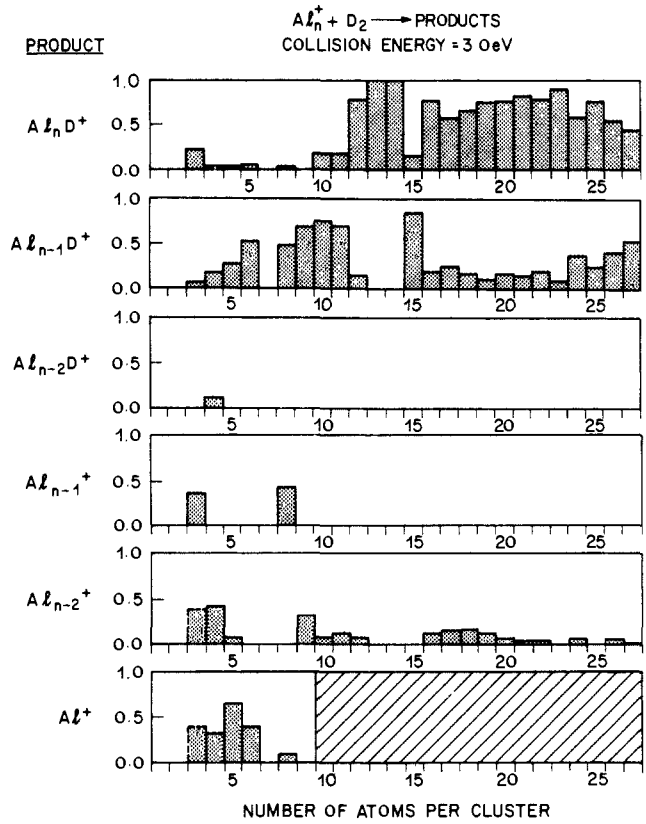

Figure 1. Product distributions recorded for the chemical reactions between aluminum cluster ions and D_2 with a collision energy of 3.0 eV. The dashed boxes show products with an ambiguous assignment; for example, Al^+ from Al_3^+ could also be classified as the Al_{n-2}^+ product.

A. Product Distributions at a Collision Energy of 3.0 eV. The product distributions recorded with a collision energy of 3.0 eV are shown in Figure 1 for aluminum clusters with between 3 and 27 atoms. There are three products formed with significant intensity over the cluster-size range studied: Al_nD^+, $Al_{n-1}D^+$, and Al_{n-2}^+. A significant amount of Al^+ is observed for the smaller clusters. As we describe below, the chemical reactions between the aluminum clusters and deuterium have significant collision energy thresholds, which is why the data reported in Figure 1 were recorded with the relatively high collision energy of 3.0 eV. Because of the large mass difference between the aluminum clusters and deuterium, this collision energy (which is in the center of mass frame) results in very large cluster ion beam laboratory energies (up to 550 eV for Al_{27}^+). The product ions have a nominal laboratory energy of approximately

$$E_p = (m_p/m_r)E_r \quad (1)$$

where E is the laboratory energy, m is the mass and the subscripts refer to reactant and product ions. Thus the low mass products, such as Al^+, have low laboratory energies. For clusters larger than Al_9^+, at a collision energy of 3.0 eV, the Al^+ product has insufficient kinetic energy to be transmitted through the second quadrupole. Thus we could not detect Al^+ from the larger clusters if any of this product were formed. Our previous work with aluminum cluster ions suggests that formation of significant amounts of Al^+ product is unlikely for the larger clusters because the drop in ionization potential which occurs with increasing cluster size favors placing the charge on the larger cluster fragment.[11] The other observed products (i.e., those except Al^+) are quite close in mass to the reactant ion, so concerns about mass and energy discrimination in their detection are minimized, and the measured relative intensities are probably reliable to within ±50%. For the Al^+ product the measured relative intensities are probably reliable to within a factor of 2 for Al_6^+ and smaller clusters and to within a factor of 4 for Al_7^+ to Al_9^+. We give these conservative estimates of the uncertainties because it is not yet possible to directly measure the detection efficiencies.

(9) Flodström, S. A.; Petersson, L.-G.; Hagström, S. B. M. *J. Vac. Sci. Technol.* **1976**, *13*, 280.
(10) Pellerin, F.; LeGressus, C.; Massignon, D. *Surf. Sci.* **1981**, *111*, L705.
(11) Ruatta, S. A.; Hanley, L.; Anderson, S. L. *Chem. Phys. Lett.* **1987**, *137*, 5.
(12) Fayet, P.; McGlinchey, M. J.; Woste, L. W. *J. Am. Chem. Soc.* **1987**, *109*, 1733.
(13) Jarrold, M. F.; Bower, J. E.; Kraus, J. S. *J. Chem. Phys.* **1987**, *86*, 3876.
(14) Jarrold, M. F.; Bower, J. E. *J. Chem. Phys.* **1987**, *87*, 1610.

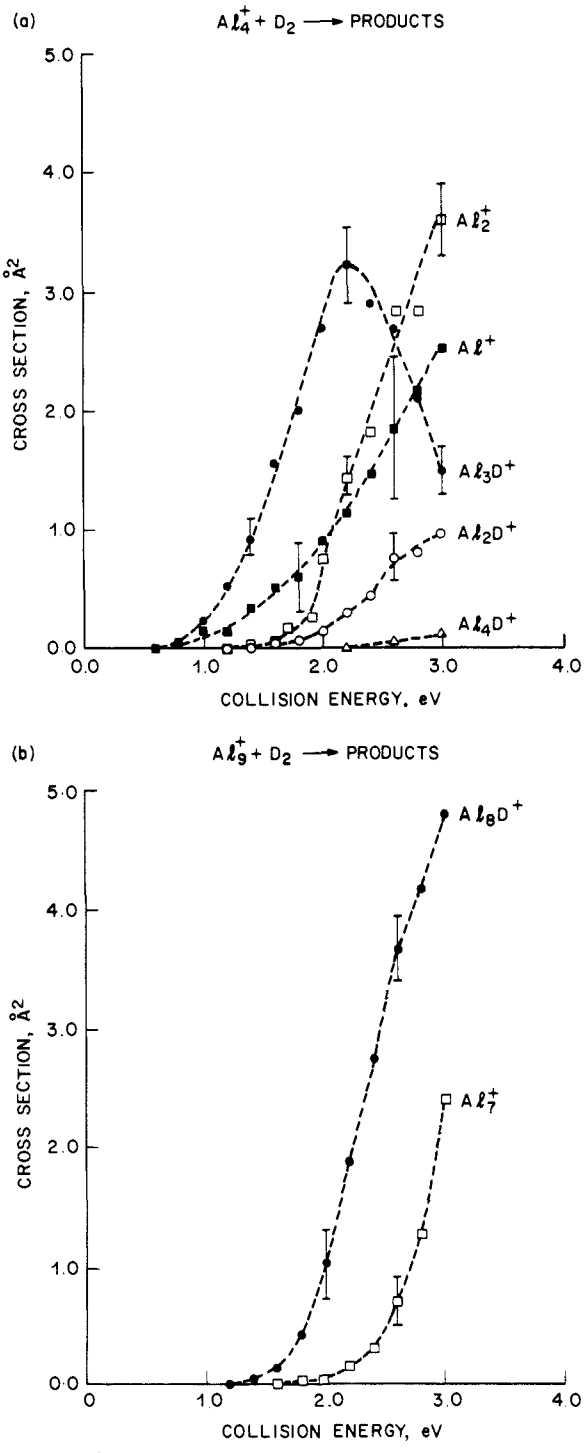

Figure 2. Collision-energy dependence of the cross sections for the main products from the reactions between (a) Al_4^+ and D_2 and (b) Al_9^+ and D_2. Error bars are shown to give an indication of the reproducibility of these measurements.

From Figure 1 we see that the main products observed from the smaller clusters (Al_3^+–Al_6^+) are $Al_{n-1}D^+$ and Al^+. Al_7^+ does not react at this collision energy. For Al_8^+–Al_{11}^+ the main products is $Al_{n-1}D^+$. For Al_{12}^+ and the larger clusters, the main product is generally Al_nD^+ with smaller amounts of $Al_{n-1}D^+$ being produced. It is clear from Figure 1 that Al_{15}^+ stands out as an exception. The main product from Al_{15}^+ is $Al_{14}D^+$. A count of valence electrons for $Al_{14}D^+$ using the jellium model[15,16] indicates that this cluster ion has a closed electronic shell configuration with

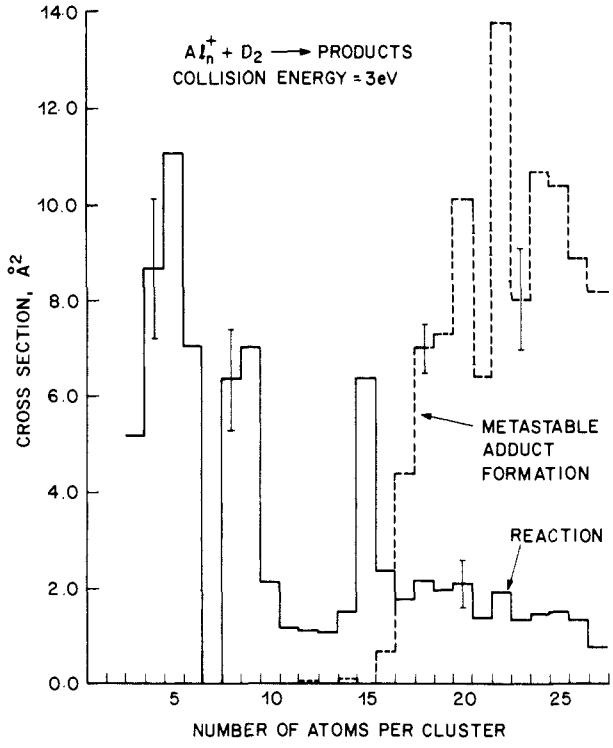

Figure 3. Total reaction cross sections (solid line) as a function of cluster size for the reactions of aluminum cluster ions with D_2 at a collision energy of 3.0 eV. Cross sections for metastable adduct formation (dashed line) are also shown for a collision energy of 3.0 eV. Error bars give an indication of the reproducibility of the measurements.

40 valence electrons.[17,18] Thus $Al_{14}D^+$ may be a particularly stable species which could account for its favored status as a product from the reaction between Al_{15}^+ and D_2.

B. Collision Energy Dependence of the Reactivity of the Smaller Clusters. We have measured the cross sections as a function of collision energy for the reactions of the smaller clusters (Al_3^+–Al_9^+) with D_2. The results for the products from Al_4^+ and Al_9^+ reactions are shown in Figure 2. The data for the other clusters show the same general features. From Figure 2 it can be seen that there are kinetic energy thresholds associated with the chemical reactions. In the case of Al_4^+ (Figure 2a), Al_3D^+ and Al^+ appear to have the lowest energy thresholds. As the collision energy is raised, the cross section for Al_3D^+ production increases to a maximum and then falls, and additional products appear, namely, Al_2D^+ and Al_2^+. For Al_9^+ (Figure 2b) the Al_8D^+ product has the lowest energy threshold. At higher collision energies an additional product appears, Al_7^+. For both Al_4^+ and Al_9^+ the $Al_{n-1}D^+$ product has the lowest energy threshold. This is a general result; the $Al_{n-1}D^+$ product has the lowest energy threshold for all the clusters studied. It seems likely that the neutral product associated with the $Al_{n-1}D^+$ ion is AlD rather than separated Al and D atoms. AlD is quite strongly bound (2.95 eV[19–21]). Notice that in Figure 2a the fall in the cross sections for Al_3D^+ correlates quite well with the increase in the higher energy products. This result suggests that the Al_2D^+ and Al_2^+ products may arise from Al_3D^+ which has sufficient internal energy to dissociate further with the

(15) Ekardt, W. *Phys. Rev. B* **1984**, *29*, 1558.
(16) Knight, W. D.; Clemenger, K.; de Heer, W. A.; Saunders, W. A.; Chou, M. Y.; Cohen, M. L. *Phys. Rev. Lett.* **1984**, *52*, 2141.

(17) The shell closing with 40 valence electrons is particularly prominent in jellium model calculations.[18] Aluminum is trivalent so Al_{14} has 42 valence electrons, removing one for the positive charge and assigning another to the Al–H bond leaves 40 valence electrons in cluster orbitals. We have had some success using this type of approach in accounting for the stability of oxidized aluminum clusters, $Al_nO_m^+$ (n = 3–26, m = 1, 2).[14]
(18) Chou, M. Y.; Cohen, M. L. *Phys. Lett. A* **1986**, *113*, 420.
(19) Using $\Delta H_f°_0$(AlH) = 2.69 eV;[20] $\Delta H_f°_0$(D) = 2.28 eV;[21] and $\Delta H_f°_0$(Al) = 3.36 eV[21] yields $D°_0$(AlD) = 2.95 eV.
(20) Wagman, D. D.; Evans, W. H.; Parker, V. B.; Halow, I.; Bailey, S. M.; Schumm, R. H. *Selected Values of Chemical Thermodynamic Properties*, NBS Technical Note 270-3; U.S. Government Printing Office: Washington, D.C., 1968.
(21) Rosenstock, H. M.; Draxl, K.; Steiner, B. W.; Herron, J. T. *J. Phys. Chem. Ref. Data* **1977**, *6*, Supplt 1 (Energetics of Gaseous Ions).

loss of either an Al atom or an AlD molecule. Similarly the Al_7^+ product from the reactions of Al_9^+ could arise from the further dissociation of Al_8D^+ by loss of another AlD molecule.

C. Total Cross Sections at a Collision Energy of 3.0 eV. Total reaction cross sections were derived using the expression

$$\sigma = \ln\left(\frac{I_r}{I_r + \sum I_p}\right)\frac{1}{nl} \qquad (2)$$

in which I_r and I_p are the measured intensities of the reactant and products, respectively, n is the gas cell number density, and l is the gas cell length (2.5 cm). Total reaction cross sections for Al_3^+ to Al_{27}^+ measured with a collision energy of 3.0 eV are shown in Figure 3 as the solid line. In our previous work on the collision-induced dissociation and chemical reactions of aluminum cluster ions, we found that a significant fraction of the ions were scattered out of the beam as gas was introduced into the gas cell.[13,14,27] This introduces uncertainty into the cross-section values deduced. In the present studies no significant (>10%) loss of ions was observed, presumably because of the large laboratory ion beam energies used in these experiments and small mass of deuterium.

For the small clusters (Al_3^+–Al_9^+) the reaction cross sections are quite large, except for Al_7^+ which does not react at this collision energy. The first indications of a reaction for Al_7^+ occur at a collision energy of 3.4 eV. These are endothermic reactions involving cluster fragmentation, and the unreactivity of Al_7^+ is probably related to its stability. There is now quite convincing evidence from several sources which shows Al_7^+ (which according to the jellium model[15,16] is a closed electronic shell species) to be a particularly stable cluster.[13,23,24] At Al_{10}^+ the reaction cross sections drop significantly and remain fairly small for all clusters up to Al_{27}^+, except for Al_{15}^+. The enhanced reactivity of Al_{15}^+ may be related to the stability of its main product $Al_{14}D^+$, which, as we noted above, may have a closed electronic shell configuration.

D. Metastable $Al_nD_2^+$ Adduct Formation. The most significant result of these studies is the direct observation of adduct formation or chemisorption of D_2 onto the aluminum clusters in the ion beam. As we demonstrate below, the $Al_nD_2^+$ adduct arises from a single collision process. It is not stabilized by further collisions and so has sufficient internal energy to dissociate back to the Al_n^+ and D_2 reactants. The $Al_nD_2^+$ does not dissociate before being detected (i.e., it is metastable) because the internal energy is distributed among the large number of internal degrees of freedom in the clusters. We have pointed out previously that the larger clusters, with many low-frequency vibrational modes, are likely to have very long lifetimes toward dissociation.[13,22] The observation of metastable $Al_nD_2^+$ adducts in these experiments is a rather striking demonstration of this effect.

The dashed line in Figure 3 shows the cross sections for metastable adduct formation as a function of cluster size at a collision energy of 3.0 eV. At this collision energy the cross sections for adduct formation rise sharply for clusters larger than Al_{15}^+. At lower collision energies metastable adduct formation was observed for clusters as small as Al_8^+. For clusters smaller than Al_8^+, metastable adduct formation was not observed, probably because the adduct does not survive long enough to be detected. The small clusters have relatively few internal degrees of freedom so the adduct lifetimes are expected to be quite short. Adduct formation was observed for all clusters in the size range Al_8^+–Al_{27}^+ with the exception of Al_{13}^+. Adduct formation was not observed for Al_{13}^+ at any of the collision energies studied between 0.2 and 3.0 eV.

Figure 4 shows a plot of the intensity of the metastable adduct against gas cell pressure for a number of clusters at different collision energies. The points are the experimental data and the lines are least-squares fits. Over the pressure range studied, the intensity of the metastable adduct increases linearly with pressure which indicates that the adduct arises from single collisions. A quadratic pressure dependence would indicate that stabilizing collisions are necessary to observe the adduct; clearly they are not. The small nonzero intercepts in Figure 4 are probably the result of a small systematic error in the pressure measurements. Detailed measurements of the type shown in Figure 4 were only performed for Al_{10}^+, Al_{16}^+, and Al_{25}^+. However, checks of the pressure dependence were routinely performed for other cluster sizes by monitoring the adduct intensity at two pressures.

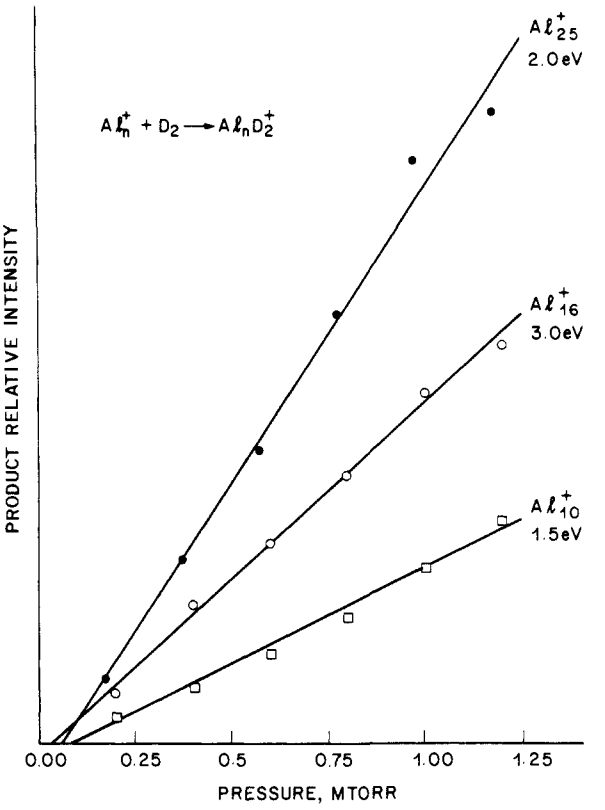

Figure 4. Plot of the intensity of the metastable adduct against gas cell pressure for Al_{25}^+ (●), Al_{16}^+ (○), and Al_{10}^+ (□) at collision energies of 2.0, 3.0, and 1.5 eV, respectively. The points are the experimental data and the lines are least-squares fits.

Figure 5 shows plots of the collision-energy dependence of the cross sections for metastable adduct formation with Al_{25}^+, Al_{16}^+, and Al_{10}^+. The points are the experimental data and the lines are least-squares fits of a model which will be discussed below. For Al_{25}^+ (Figure 5a) the cross sections for adduct formation show a threshold and then increase steadily over the collision-energy range studied. The cross sections for Al_{16}^+ (Figure 5b) also show a threshold; they then increase to a maximum at around 2.3 eV and decline with increasing collision energy. It seems likely that the falloff in the cross sections at higher collision energies results from unimolecular dissociation of the adduct before it is detected. This occurs at the highest collision energies because the adduct contains more internal energy, and lifetimes toward dissociation are expected to decrease with increasing internal energy. The cross sections for Al_{10}^+ (Figure 5c) shows the same general features. They rise from a threshold to a maximum at around 1.6 eV and then fall approaching zero at a collision energy of 2.7 eV. Al_{10}^+ has fewer internal degrees of freedom than Al_{16}^+, and clearly the data for Al_{10}^+ are more strongly influenced by the unimolecular dissociation of the adduct before detection. Notice the substantial drop in the size of the cross sections for metastable adduct formation on going from Al_{16}^+ to Al_{10}^+. Clearly for Al_{10}^+, clusters with only a relatively narrow range of energies above the threshold are metastable long enough to be detected.

IV. Analysis of the Threshold Data

It seems natural to relate the thresholds observed for adduct formation to the activation barrier associated with chemisorption; therefore, accurate values for the thresholds are of considerable interest. The analysis of the threshold region for chemical reactions

(22) Jarrold, M. F.; Bower, J. E. *J. Chem. Phys.*, in press.
(23) Begemann, W.; Dreihofer, S.; Meiwes-Broer, K. H.; Lutz, H. O. In ref 7.
(24) Hanley, L.; Ruatta, S. A.; Anderson, S. L. *J. Chem. Phys.* **1987**, *87*, 260.

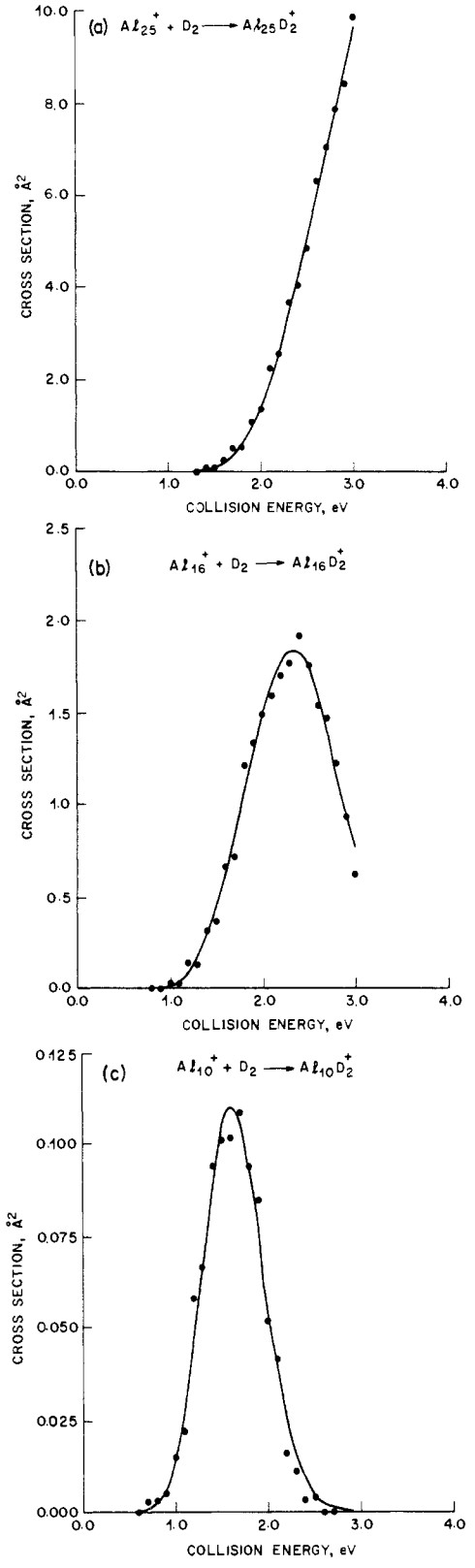

Figure 5. Plots of the cross sections for adduct formation against collision energy for (a) Al_{25}^+, (b) Al_{16}^+, and (c) Al_{10}^+. The points are the experimental data and the lines are the result of a nonlinear least-squares fit to derive the thresholds (see text).

studied using beam techniques is a well-understood problem.[24-28] A similar approach can be employed to analyze the threshold

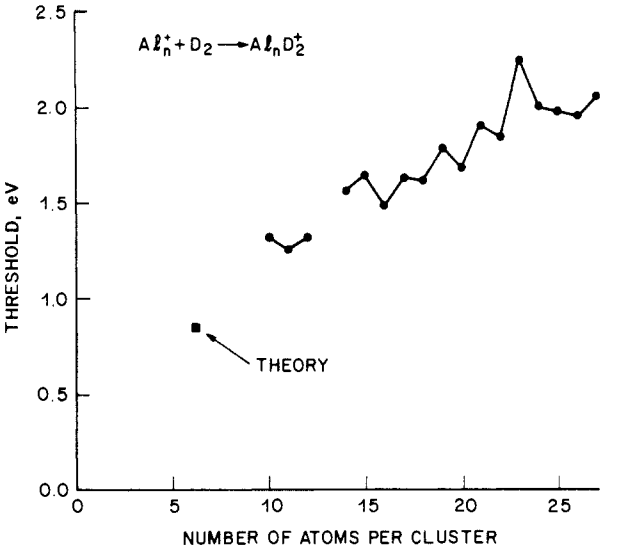

Figure 6. Plot of the thresholds for adduct formation against cluster size. The estimated uncertainties are not shown in the figure for clarity but are given in Table I. The line joining the data points is only a guide to emphasize the oscillatory behavior. The point labeled theory is taken from ref 7.

region for metastable adduct formation. In order to determine thresholds from the experimental data, it is necessary to account for the broadening of the threshold region that arises from thermal motion of the target gas and the kinetic energy spread of the ion beam. With the ion–neutral mass ratios for the experiments reported here, virtually all the threshold broadening arises from thermal motion of the target gas. The method generally used to account for the broadening of the threshold region[24-28] involves convolution of an assumed cross-section function with a function to describe the threshold broadening. We assumed a cross-section function of the form

$$\sigma(E) = A(E - E_0)^n \exp[-k(m,E - E_0)t] \qquad (3)$$

for $E > E_0$ and with $n = 1$. The first term in this expression generates a linear increase in cross section (with slope A) from the threshold E_0. From the data shown in Figure 5 for Al_{25}^+, it is clear that a model assuming a linear dependence of the cross section on collision energy is a good approximation. The second term in eq 3 accounts for the unimolecular dissociation of the adduct before detection. $k(m,E - E_0)$ is the rate constant for dissociation and t is the time the adduct must survive in order to be detected. This time is assumed to be the flight time from the center of the gas cell to the middle of the second quadrupole,[29] which is typically around 40 μs and is dependent on the collision energy and cluster size. $k(m,E - E_0)$ is given by

$$\log k(m,E - E_0) = m(E - E_0 + a) - b \qquad (4)$$

where m is an adjustable parameter and a and b are constants selected to fit calculated RRKM rate constants for dissociation of the adduct in the lifetime range of interest, assuming dissociation of the adduct occurs by desorption of a deuterium molecule.[30,31]

(25) Chantry, P. J. *J. Chem. Phys.* **1971**, *55*, 2746.
(26) Liftshitz, C.; Wu, R. L. C.; Tiernan, T. O.; Terwilliger, D. T. *J. Chem. Phys.* **1978**, *68*, 247.
(27) Armentrout, P. B.; Beauchamp, J. L. *J. Chem. Phys.* **1981**, *74*, 2819.
(28) Ervin, K. M.; Armentrout, P. B. *J. Chem. Phys.* **1985**, *83*, 166.
(29) We arbitrarily assume that $Al_nD_2^+$ adducts that survive long enough to get over halfway through the quadrupole will be transmitted as $Al_nD_2^+$.
(30) The vibrational frequencies of the clusters required for the RRKM calculation were estimated using the simple model we have described previously.[22] For the frequencies of the Al–D modes in the adduct we used the frequencies of C–D stretches and bends in hydrocarbons.[31] For the transition state one of the Al–D stretches was taken as the reaction coordinate. Of the other five Al–D modes one of the bends was assumed to become the D_2 stretch in the separated products and the other four vibrational modes vanish as the products separate. We calculated RRKM rate constants for a range of cluster sizes, transition-state parameters, binding energies, and cluster vibrational frequencies. We then selected a and b to fit the calculated rates in the lifetime range relevant to the experiment. One set of values for a and b is sufficient to adequately fit the calculated rates for all cluster sizes. A plot of log k against $E - E_0$ is not linear (see the plots given in ref 22); however, for our application we can use a linear approximation because we only need accurate values for the rates of dissociation over a narrow energy range.

Table I. Thresholds and Other Parameters Used To Fit the Experimental Data for Clusters in the Size Range n = 10–27

cluster size	threshold, eV	fitting parameters A	fitting parameters m
10	1.32 ± 0.30	1.15	9.55
11	1.26 ± 0.30	2.29	9.03
12	1.32 ± 0.25	2.78	6.61
13			
14	1.57 ± 0.25	1.96	5.77
15	1.65 ± 0.30	1.51	8.63
16	1.48 ± 0.20	2.98	4.64
17	1.63 ± 0.20	5.25	3.87
18	1.62 ± 0.20	7.48	3.69
19	1.79 ± 0.20	6.80	3.39
20	1.69 ± 0.20	9.82	3.48
21	1.91 ± 0.20	6.52	3.70
22	1.85 ± 0.15	11.17	NR[a]
23	2.25 ± 0.15	9.61	NR
24	2.01 ± 0.15	10.08	NR
25	1.99 ± 0.15	9.62	NR
26	1.96 ± 0.15	7.98	NR
27	2.06 ± 0.15	8.28	NR

[a] Not required.

Equation 3 was fit to the experimental data with a nonlinear least-squares procedure, using the convolution integral of Chantry[25] to account for target gas motion and a numerical integration over a Gaussian to account for the ion beam energy spread. Examples of the resulting fits are shown in Figure 5. Average values of the thresholds derived from the experimental data in this way are shown plotted as a function of cluster size in Figure 6. The thresholds with estimated uncertainties, along with averages of the other parameters used to fit the experimental data (A and m), are tabulated in Table I. Thresholds were only derived for clusters in the size range n = 10–27 (except for Al_{13}^+). Although adduct formation was observed for n = 8 and 9, the cross sections were too small for reliable thresholds to be obtained.

There are several potential sources of error with the thresholds arising from both experimental factors and the assumptions made in analyzing the data. One question concerning the experimental data is whether or not the measured intensities of Al_n^+ and $Al_nD_2^+$ species reflect their true intensities. Although the intensities were recorded with a relatively high mass resolution (around 2 amu fwhm), the product and reactant ions are sufficiently close in mass for it to be difficult to believe that there could be any significant mass discrimination either in the analyzing quadrupole or at the detector. To avoid any potential problems the instrument was carefully refocused at every new collision energy. Another factor which we have considered is the ion beam energy spread. We currently use a simple retarding potential energy analyzer to determine the ion beam energy distribution.[13] The measured distributions are dominated by the resolution of the energy analyzer which is typically around 3 eV,[32,33] and so the true distribution is not precisely known. However, for these experiments accurate knowledge of the ion beam energy spread is not required as it virtually vanishes in the center of mass frame because the mass of the ion is much larger than that of the neutral. Analysis of the threshold data assuming a Gaussian ion beam energy distribution with a 0.1-eV fwhm and 3.0-eV fwhm resulted in threshold values differing by only a few meV. Gas cell pressure is another factor which should be considered. The majority of the experimental data were recorded with a gas cell pressure of approximately 1.0 mtorr. To ensure that gas cell pressure in no way influenced the measured thresholds, a substantial fraction of the experimental data was also recorded with a gas cell pressure of 0.25 mtorr. There appeared to be no statistically significant difference between the data sets recorded with these two pressures.

The other potential sources of error with the derived thresholds arise from assumptions made in analyzing the data. The first assumption we consider is that of a linear dependence of the cross sections on collision energy. From the experimental data shown in Figure 5 it is clear that this appears to be a valid assumption for the larger clusters. If the assumption of a linear cross section is relaxed for the larger clusters (Al_{22}^+–Al_{27}^+) and we refine n (see eq 3) in the least-squares analysis, n generally converges to a value close to 1.0. We also fit some data sets using $A(E - E_0)^n/E$ rather than $A(E - E_0)^n$ (with n being refined), and it made no significant difference to the derived thresholds. While the linear cross-section assumption appears valid for the larger clusters, for clusters smaller than Al_{22}^+ the cross sections are influenced by unimolecular dissociation of the adduct before detection, and it is not possible to determine whether the linear cross-section assumption is valid.

For the smaller clusters, including the term to account for the unimolecular dissociation of the adduct introduces an additional source of uncertainty. For clusters strongly influenced by adduct dissociation, a relatively wide range of values for A and m provide comparable (at least to the eye) fits to the experimental data. Fortunately the thresholds derived by fixing either A or m and refining the other along with E_0 do not vary by a large amount, and we include this potential source of error in our estimates of the uncertainties. One other factor which needs to be considered is the reliability of eq 4 which accounts for the unimolecular dissociation of the adduct. We assumed that dissociation of the adduct occurs by desorption of deuterium. However, we also observe the products of chemical reactions which could arise from adduct dissociation. So there is a chance that desorption of deuterium is not the lowest energy dissociation pathway of the adduct. This possibility was investigated by fitting a few data sets using the expression

$$\log k(m,E - E_0) = m(E - E_0 + a + E_x) - b \qquad (5)$$

where E_x is taken to be the energy difference between the activation energy for the product and the desorption energy for deuterium. E_x was stepped in units of 0.2 eV. We found that values of E_x of up to 1.0 eV generated comparable fits to the experimental data with no significant difference in the thresholds (the change in E_x was accommodated mainly by a change in the value of m). So eq 4 provides a sufficiently accurate way to account for the unimolecular dissociation of the adduct.

Total estimated uncertainties in the threshold values are given in Table I. They are not reproduced in Figure 6 for clarity. The estimated uncertainties contain contributions from the statistical scatter in the experimental data (reproducibility of the threshold values) as well as uncertainties that arise from the fitting procedure. The uncertainties are larger for the smaller clusters owing to the unimolecular dissociation of the adduct which results in larger uncertainties in the fitting procedure.

As can be seen from the plot of the thresholds in Figure 6, they show an overall increase with cluster size, going from a little over 1 eV to around 2 eV. For clusters with n = 14 and larger, there is a clear odd–even alternation in the size of the thresholds. The clusters with an odd number of atoms have larger thresholds. The threshold for Al_{23}^+ is particularly large. The odd–even oscillations are generally within our uncertainties given in Table I. However, these oscillations were quite reproducible and so it seems likely that they are real features.

V. Discussion

A. Significance of the Thresholds. As mentioned above, it seems natural to relate the thresholds determined for metastable adduct formation to the activation barriers for chemisorption of deuterium onto the clusters. However, there are several caveats that must be mentioned. Ideally, threshold measurements provide an upper limit; in other words, the activation barriers could be smaller than the thresholds but not larger. How close the threshold measurement comes to the true activation barrier depends on the nature of the potential surface and the transition state. In our

(31) Shimanouchi, T. *Tables of Molecular Vibrational Frequencies*, Consolidated Vol. 1; NSRDS-NBS39; U.S. Government Printing Office: Washington, D.C., 1972).

(32) Our simple retarding potential energy analyzer consists of three plates containing apertures covered by a fine mesh grid. The stopping potential is placed on the middle electrode. The energy resolution is limited by field penetration through the grid apertures.[33]

(33) Jones, R. *Rev. Sci. Instrum.* **1978**, *49*, 23.

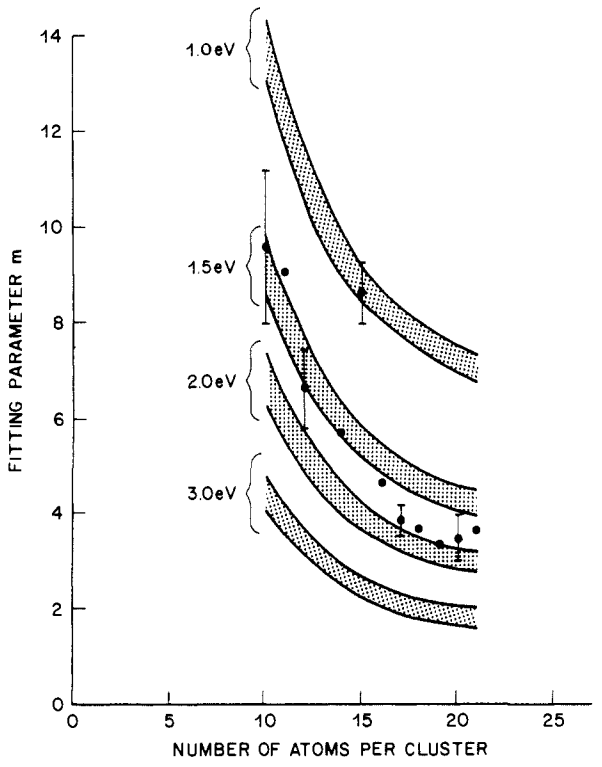

Figure 7. Plot of the parameter m against cluster size. The shaded regions are the result of RRKM calculations for a range of desorption energies which are discussed in the text. The parameter m was not required to fit the cross-section data for clusters with $n > 21$. Error bars are shown to give an indication of the reproducibility of values of m determined from different data sets.

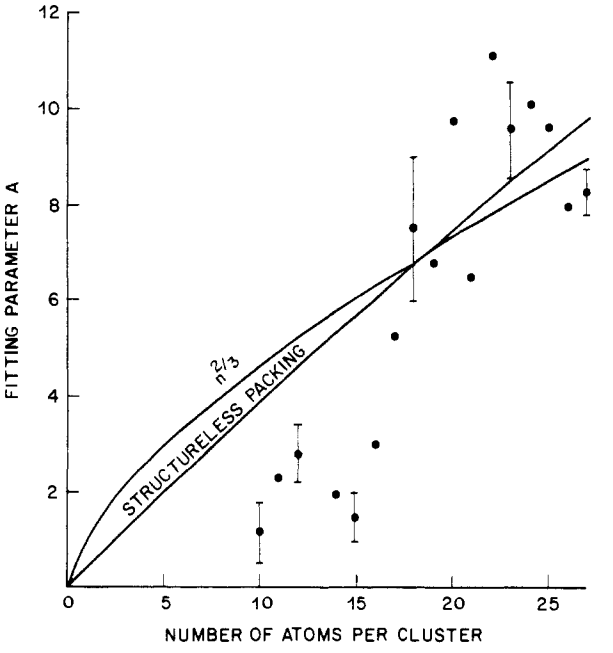

Figure 8. Plot of the parameter A against cluster size. A is derived from a least-squares fit to the cross sections for adduct formation (see text). Error bars are shown to give an indication of the reproducibility of the values of A determined from different data sets.

experiment we are driving the chemisorption process with kinetic energy. As should be apparent from the work of Polanyi,[34] it is possible (for example) that driving the chemisorption by vibrational excitation of the deuterium could be more effective. If this were true, then there is a chance that the thresholds we derive will be larger than the true activation barriers.

Internal energy in the clusters could result in low threshold values. As we have discussed in some detail elsewhere,[13] the clusters undergo a large number of collisions (an average of 10^5) after ionization and before exiting the source, and they probably reach thermal equilibrium with the buffer gas which is at a temperature of around 135 K.[35] If thermal equilibrium is not achieved it seems likely that any small residual amount of excess energy will be spread over the large number of degrees of freedom in the cluster and have negligible impact on the threshold values.

In conclusion then, it appears reasonable to relate the measured thresholds to the activation barriers for chemisorption of deuterium onto the clusters, but one should keep in mind the potential problems mentioned above.

B. Significance of the Parameters A and m. The parameter m used to fit the experimental data on the thresholds for metastable adduct formation accounts for the unimolecular dissociation of the adduct before detection. As described above m is related to the rate constant for unimolecular dissociation (see eq 4). Since the dissociation rate is a rather sensitive function of the dissociation energy, it is in principle possible to derive an estimate for the desorption energy of D_2 (the activation energy for the desorption of D_2 from the clusters) from these data (assuming that this is the lowest energy dissociation pathway). Unfortunately, more factors than the dissociation energy influence the rates of unimolecular dissociation (for example, the properties of the transition state). Also we noted above that for the smaller clusters a relatively wide range of values for A and m produce comparable fits to the experimental data so the values of A and m for some of the smaller clusters may not be very well defined. Furthermore, it is not certain that desorption of deuterium is the lowest energy dissociation pathway for all the adducts, so determining accurate values for the desorption energies from these data is not practical. However, we can use these data to crudely bracket the desorption energies. Figure 7 shows a plot of the parameter m against cluster size. The points are the experimental data and the shaded regions are the result of RRKM calculations for the rates of dissociation with a range of desorption energies from 1.0 to 3.0 eV. The shaded regions give an indication of the sensitivity of the calculations to the input parameters (they represent the range of values obtained by varying the transitional modes in the transition state from 75 to 25% of their change on going from reactants to products).

As can be seen in Figure 7, the desorption energy for $Al_{10}D_2^+$, $Al_{11}D_2^+$, and $Al_{15}D_2^+$ is 1.0–1.5 eV, and for all the other clusters it is 1.5–2.0 eV. The parameter m was not required to fit the experimental data for clusters with $n > 21$, so no information on the desorption energies can be deduced for the larger clusters. As can be seen from Figure 7 the desorption energy deduced for $Al_{15}D_2^+$ is particularly small. Al_{15}^+ has a large cross section for reaction (see Figure 3), and it is likely that desorption of deuterium (D_2) is not the lowest energy dissociation pathway for this cluster. The lowest energy dissociation pathway is probably formation of $Al_{14}D^+$ (see Figure 1) which may have a closed electronic shell configuration. Thus the "desorption energy" deduced for $Al_{15}D_2^+$ is probably the activation energy for loss of AlD, and this is less than the desorption energy for deuterium for this particular cluster because of the stability of $Al_{14}D^+$. For the other clusters it is likely that loss of deuterium (D_2) is the lowest energy dissociation pathway of the metastable adduct. Desorption energies of the magnitude found here are consistent with dissociative chemisorption rather than physisorption (where molecular deuterium is weakly bound to the cluster). However, note that the estimated desorption energies and the activation barriers for chemisorption are comparable, so the $Al_nD_2^+$ adduct is only weakly bound relative to separated $Al_n^+ + D_2$, if it is bound at all.

The parameter A describes the rate of increase of the cross sections with collision energy. This is related to the magnitude of the cross sections and so we might anticipate that this parameter could provide information on the number of equivalent binding sites for deuterium on the cluster. A plot of the parameter A

(34) See, for example: Polanyi, J. C. *Science* **1987**, *236*, 680.

(35) Further cooling could occur in the expansion. But since the kinetic, rotational, and vibrational degrees of freedom are not cooled to the same extent and the expansion is quite mild, use of the gas temperature as an upper limit seems appropriate.

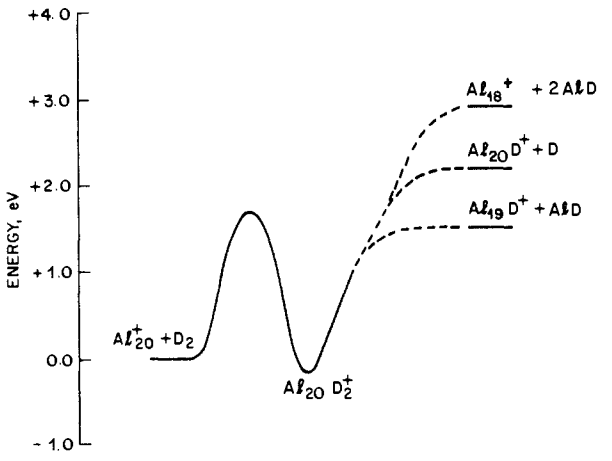

Figure 9. Schematic potential energy diagram for the $Al_{20}^+ + D_2$ system. The energetics are probably reliable to within ±0.5 eV.

against cluster size is shown in Figure 8. The line in Figure 8 labeled structureless packing gives the number of surface atoms using the structureless packing model of Riley and co-workers.[36] The line labeled $n^{2/3}$ in Figure 8 gives the variation of the cross-sectional area of the cluster (i.e., the size of the cluster as a target looking from the deuterium molecule). The normalization of both lines relative to the experimental data is arbitrary. While both the experimental data and the lines due to the simple models increase with cluster size, the agreement between the data and the predictions of both models is not very good.

C. Chemical Reactions between the Clusters and Deuterium. In addition to adduct formation we observed chemical reactions between the clusters and deuterium. We deal first with the larger clusters, with $n \geq 10$. For the larger clusters two main products were observed, Al_nD^+ and $Al_{n-1}D^+$. As we discussed above, it seems likely that an AlD molecule is the neutral product associated with $Al_{n-1}D^+$. In Figure 9 we show a schematic potential-energy diagram constructed for Al_{20}^+ (as an example) using the information deduced from the threshold data along with the dissociation energy of D_2 (4.56 eV[21]), the dissociation energy of AlD (2.95 eV[19]), and assuming that aluminum atoms are bound to the cluster by 2.15 eV.[37,38] The estimated energies given in Figure 9 are probably reliable to within ±0.5 eV. As can be seen from Figure 9 the lowest energy product is $Al_{n-1}D^+ + AlD$, followed by $Al_nD^+ + D$. However, for the product distributions measured with a collision energy of 3.0 eV, generally more Al_nD^+ than $Al_{n-1}D^+$ is observed for the larger clusters. This result suggests that either there is a barrier associated with loss of AlD from the $Al_nD_2^+$ adduct or that some of the Al_nD^+ product arises from a direct reaction that does not involve the $Al_nD_2^+$ adduct as an intermediate (for example, a spectator stripping mechanism). It seems likely that formation of the $Al_{n-1}D^+$ product requires the involvement of an $Al_nD_2^+$ intermediate because formation of this product requires significantly more reorganization of the bonding. Note that the $Al_{n-1}D^+ + AlD$ products are slightly lower in energy than $Al_n^+ + D_2$ in Figure 9. However, since the reaction cross sections are so small for the larger clusters, and the main product is Al_nD^+, it seems likely that the lowest energy dissociation pathway of the $Al_nD_2^+$ adduct is loss of D_2 (as assumed above) except in the case of $Al_{15}D_2^+$.

We will now consider the smaller clusters, with $n < 10$. For these clusters three main products are observed: $Al_{n-1}D^+$, Al_{n-2}^+, and Al^+. As we have discussed above, the $Al_{n-1}D^+$ and Al_{n-2}^+ products can be accounted for by the loss of AlD molecules from the $Al_nD_2^+$ complex. Al^+ is the main product in the collision-induced dissociation of these smaller clusters by argon and xenon,[13,24] and it probably arises from collision-induced dissociation here as well since neutral Al_nD_2 are not observed in the experiments of Cox and co-workers[7] for $n < 6$. The Al_{n-1}^+ product observed for Al_3^+ and Al_8^+ also probably arises from collision-induced dissociation; losses of an atom from both Al_3^+ and Al_8^+ are important processes in the collision-induced dissociation of these clusters by argon.[13] There is no evidence for the collision-induced dissociation of the larger clusters (which results in Al_{n-1}^+[13]) probably because they are more strongly bound and also require more excess energy to dissociate in the experimental time frame.

In principle it is possible to extract threshold information for the smaller clusters from the kinetic energy dependence of the reaction cross sections (Figure 2). We did, in fact, determine some threshold values in the early stages of this work. However, it quickly became apparent that the physical significance of these threshold values was not clear. They could be due to reaction endothermicity or activation barriers, and there is insufficient thermodynamic information available at present to be able to say which is responsible, so this work was not pursued further. Note that this is not the case when the adduct is directly observed as reported here for the larger clusters. Then the thresholds can unambiguously be assigned to an activation barrier.

D. Activation Barriers for Chemisorption of Deuterium. There are two significant points about the threshold data shown in Figure 6. First, the thresholds or activation barriers increase with[39] cluster size; and, second, there is a clear odd–even alternation in the height of the activation barriers for clusters with $n > 13$. As we noted in the Introduction, chemisorption of hydrogen on *neutral* aluminum clusters has been observed for only $n = 6$ and 7. It does not occur to any significant extent for clusters with more than seven atoms. Our results show the presence of substantial activation barriers for chemisorption on aluminum cluster *ions* with $n = 10$–27. These activation barriers are sufficiently large that the rate constant for chemisorption on the larger clusters at room-temperature kinetic energies will be effectively zero. So the available data on the small neutral clusters and large ionic clusters appear to be consistent, although it is not clear to what extent the reactivity of neutral and ionic metal clusters are expected to be related. Calculations by Upton,[7] discussed in more detail below, suggest that the charge only has a minor influence.

Chemisorption of hydrogen (H_2) on polycrystalline aluminum surfaces has not been observed.[9,10] It is tempting to suggest that the failure to observe chemisorption on bulk aluminum is related to the activation barriers discovered in this work. In fact, from the data shown in Figure 6 the activation barriers tend to saturate with increasing cluster size toward a level which could be the bulk activation barrier.

In experiments in which H *atoms* are adsorbed on an aluminum surface at low temperatures, desorption of hydrogen molecules is observed at temperatures above 80 K.[40] This result suggests that hydrogen is only weakly bound to the aluminum surface, with an activation energy for desorption of around 0.2 eV. This is significantly smaller than the desorption energies deduced for the clusters. Recent calculations on the chemisorption of hydrogen on an Al_{13} cluster suggest that the H atoms may penetrate into the cluster and cause substantial expansion of the cluster lattice. Perhaps hydrogen is more strongly bound to the clusters than the bulk because the H atoms are easily able to penetrate the cluster lattice. There may be a barrier to penetration of the bulk lattice and the resulting expansion of the lattice is clearly more difficult

(36) Parks, E. K.; Liu, K.; Richtsmeier, S. C.; Pobo, L. G.; Riley, S. J. *J. Chem. Phys.* **1985**, *82*, 5470.

(37) Derived using the semiempirical model of Freund and Bauer[38] which gives the cluster cohesive energy as $\Delta H_n = n\Delta H_\infty(1 - n^{-0.25})$ in which ΔH_∞ is the bulk cohesive energy per atom. This estimate is probably reliable to within ±0.5 eV on average. Note that this expression gives the cluster cohesive energy. The dissociation energy of cluster n is thus $D^\circ_n = \Delta H_n - \Delta H_{n-1}$ for the process $n \rightarrow n - 1$.

(38) Freund, H. J.; Bauer, S. H. *J. Phys. Chem.* **1977**, *81*, 994.

(39) A referee, noting that the increase in chemisorption threshold is unexpected, suggested that this increase could be due to the reaction cross sections increasing more slowly as the reactants get larger. This has been observed in the reactions of atomic ions with H_2 and C_2H_4. For the reactions studied here the reverse appears to be true. The cross sections rise more rapidly for the larger clusters (see Figure 8). In any case the thresholds are derived from computer simulations of the experimental data and are independent of the rate that the cross sections rise above the threshold.

(40) Hayward, D. O.; Trapnell, B. M. W. *Chemisorption*; Butterworths: London, 1964; p 233.

to accommodate. Jellium model calculations of H atom chemisorption on bulk aluminum suggest the existence of a substantial barrier (1.2–1.4 eV) to hydrogen atom migration into the bulk.[42]

There have been several attempts to understand chemisorption of hydrogen (H_2) on organometallic complexes, clusters, and metal surfaces from a theoretical point of view.[6,7,41-47] The critical factors that emerge from these studies are that M(HOMO) → $H_2(\sigma^*)$ and $H_2(\sigma)$ → M(LUMO) (where M is an organometallic complex, cluster or surface) electron transfer can play a role in activating the H_2 and facilitating H_2 bond cleavage, and that reorganization of the molecular orbitals on M to accommodate the M–H bonds is also important. Saillard and Hoffmann[44] have suggested that the $H_2(\sigma)$ → M(LUMO) transfer is probably important for some organometallic complexes, but the M(HOMO) → $H_2(\sigma^*)$ transfer dominates for surfaces.

Upton has performed a detailed theoretical study of chemisorption of hydrogen on Al_6.[6,7] His calculations suggest that both M(HOMO) → $H_2(\sigma^*)$ and $H_2(\sigma)$ → M(LUMO) transfer occurs but with M(HOMO) → $H_2(\sigma^*)$ winning on balance. Whether or not M(HOMO) → $H_2(\sigma^*)$ dominates may be unimportant because Upton's calculations also suggest that, although electron transfer plays an important role in weakening the H_2 bond, it is probably not the main factor in determining the size of the activation barrier. The main factor appears to be changes in the population of the cluster molecular orbitals in order to minimize repulsive interactions and form the new M–H bonds. Upton calculated activation barriers of 0.78 and 0.86 eV for chemisorption of D_2 on neutral and cationic Al_6. The calculated activation barrier for Al_6^+ is plotted in Figure 6, and it is apparent that our experimental data extrapolate quite nicely to the calculated value. However, the calculated activation barrier of 0.78 eV for neutral Al_6 seems a little too high for chemisorption to occur with any significant efficiency at close to room temperature in a fast-flow reactor experiment.[7]

If, as discussed above, the activation barrier arises from changes in the population of the cluster molecular orbitals to minimize repulsive interactions, then the activation barrier might be expected to *decrease* with cluster size because as the cluster size increases the electronic density of states increases, and so the promotion energy to a state of the required symmetry would be expected to fall. We observe an *increase* in the activation barrier with cluster size.[39] Unfortunately there have been no detailed calculations for hydrogen chemisorption on larger aluminum clusters. Some calculations have been reported for Al_{13},[35] but the authors did not consider the activation barrier. They found relatively weak Al–H bonds (0.92 eV per H atom). Al_{13}^+ was the only cluster (except the smallest ones) for which we did not observe adduct formation so Al_{13} does not seem to be typical. There are no detailed calculations on hydrogen chemisorption on larger clusters, but there have been some jellium calculations for hydrogen chemisorption[46] on several free-electron metals including aluminum. Although not as accurate as high-quality ab initio calculations, the trends predicted by these calculations appear to be in reasonable agreement with the available experimental data. The calculations for H_2 chemisorption on aluminum found a barrier in excess of 1.3 eV for chemisorption and a desorption energy of a few tenths of an electron volt.[46]

As can be seen from Figure 6, there is a clear odd–even alternation in the height of the activation barrier for chemisorption on clusters with $n \geq 14$. The clusters with an even number of atoms have lower activation energies. Since the clusters are singly charged, the ones with an even number of atoms have an odd number of valence electrons (aluminum is trivalent). Presumably an unpaired electron in the highest occupied molecular orbital leads to a lower activation barrier by reducing the repulsive interaction between deuterium and the clusters at the transition state. An implication of these results is that all the clusters must be low spin.

It is clear from Figure 6 that the activation barrier for Al_{23}^+ is particularly large. According to the jellium model,[15,16] Al_{23}^+ has a closed electronic shell configuration with 68 valence electrons (corresponding to the closing of the 2d shell). A closed electronic shell would be expected to result in a high activation barrier. Also note that we did not observe adduct formation for Al_{13}^+. Al_{13}^+ (with 38 valence electrons) is close to the 2p shell closing with 40 valence electrons. It is not clear whether the absence of adduct formation for Al_{13}^+ is due to a low desorption energy or large activation barrier for chemisorption, or whether this is a consequence of the 2p shell closing or due to the compact close-packed structure that Al_{13} could adopt.

VI. Conclusions

In this paper we have described the results of a detailed study of the interaction of size-selected aluminum clusters with deuterium. We observed both chemical reactions and metastable adduct formation. The metastable adduct arises from chemisorption of deuterium onto the clusters *without stabilizing collisions*. The adduct survives long enough to be detected because of the large number of low-frequency vibrational modes in the clusters.

Adduct formation was observed for all clusters in the size range $n = 8$–27 except for Al_{13}^+. Analysis of the collision-energy dependence of adduct formation provided thresholds, which were related to the activation barriers for chemisorption, and for some clusters estimates of the desorption energy (the activation energy for desorption of deuterium from the clusters).

The activation barriers increase with cluster size and show significant odd–even oscillations. The activation barriers for the odd clusters are larger than those for the even ones. We compared these results with simple models for chemisorption but could not satisfactorily account for the increase in the activation barriers with cluster size.[39] Detailed ab initio calculations may be required to uncover the origin of this increase. The lower activation barriers for the even clusters can be accounted for by the reduced repulsive interactions at the transition state due to the presence of an unpaired electron in the highest occupied molecular orbital.

In addition to adduct formation we observed chemical reactions. The reactions showed kinetic-energy thresholds, suggesting that they arise from endothermic processes. The main products observed were Al_{n-1}^+, Al_{n-2}^+, and Al^+ for clusters with $n < 10$ and Al_nD^+ and $Al_{n-1}D^+$ for the larger clusters. It is likely that the neutral products associated with $Al_{n-1}D^+$ and Al_{n-2}^+ are AlD molecules so these products are analogous to the formation of $Al_{n-4}^+ + 2Al_2O$ in the reactions with oxygen.[20] The Al^+ observed for the smaller clusters probably arises from collision-induced dissociation. Formation of $Al_{n-1}D^+$ and Al_{n-2}^+ products probably involves an $Al_nD_2^+$ intermediate, but the Al_nD^+ product could arise from a direct (stripping) mechanism since much more Al_nD^+ is observed than the lower energy $Al_{n-1}D^+$ product.

Acknowledgment. We thank Professor S. L. Anderson for helpful discussions regarding the data analysis.

(41) Partridge, H.; Bauschlicher, C. W. *J. Chem. Phys.* **1986**, *84*, 6507.
(42) Hjelmberg, H. *Surf. Sci.* **1979**, *81*, 539.
(43) Upton, T. H. *J. Am. Chem. Soc.* **1984**, *106*, 1561.
(44) Saillard, J.-Y.; Hoffmann, R. *J. Am. Chem. Soc.* **1984**, *106*, 2006.
(45) Harris, J.; Anderson, S. *Phys. Rev. Lett.* **1985**, *55*, 1583.
(46) Johansson, P. K. *Surf. Sci.* **1981**, *104*, 510.
(47) Norskov, J. K.; Houmoller, A.; Johansson, P. K.; Lundquist, B. I. *Phys. Rev. Lett.* **1981**, *46*, 257.